


Article

Stability Evaluation of Layered Backfill Considering Filling Interval, Backfill Strength and Creep Behavior

Chongchong Qi ^{1,2,*} , Li Guo ¹, Yu Wu ², Qinli Zhang ¹ and Qiusong Chen ^{1,*}

¹ School of Resources and Safety Engineering, Central South University, Changsha 410083, China; guoli1220@csu.edu.cn (L.G.); zhangqinlicn@126.com (Q.Z.)

² State Key Laboratory for GeoMechanics and Deep Underground Engineering, China University of Mining & Technology, Xuzhou 221116, China; yuwu2020@126.com

* Correspondence: chongchong.qi@csu.edu.cn (C.Q.); qiusong.chen@csu.edu.cn (Q.C.)

Abstract: Cemented paste backfill (CPB) is the primary solution to improving the safety of continuous mining. The interaction between rock mass and backfill is an important indicator of backfill stability. The creep behavior of weak rock mass is an essential factor, which causes the evolution of stresses and displacements in the backfill stope. In this paper, numerical models were constructed to analyze the interactions between rock mass and backfill by considering the creep behavior of the rock mass, filling interval, and backfill strength. The numerical simulation results showed the effects of different parameters, including the number of backfilling layers, filling interval time (FIT), and backfill strength under creep behavior on stress, displacements, and plastic deformation. The horizontal displacement near the mid-height and vertical displacement at the top of the backfilled stope is the largest compared to layered backfilling. The stress within the backfilled stope is smallest when the stope is filled in a single layer. With increasing FIT, stress in the backfilled stope decreases. FIT mainly affected the horizontal displacement of the stope. The stresses on the stope bottom decrease when the strength of the middle-backfilled stope decreases. Overall, this study provides important insights for understanding the creep behavior of rock mass in underground backfilling practices.

Keywords: backfill; time-dependent of rock mass; FLAC^{2D}; stress and displacement; a parametric study



Citation: Qi, C.; Guo, L.; Wu, Y.; Zhang, Q.; Chen, Q. Stability Evaluation of Layered Backfill Considering Filling Interval, Backfill Strength and Creep Behavior. *Minerals* **2022**, *12*, 271. <https://doi.org/10.3390/min12020271>

Academic Editor: Abbas Taheri

Received: 17 December 2021

Accepted: 17 February 2022

Published: 21 February 2022

Publisher's Note: MDPI stays neutral with regard to jurisdictional claims in published maps and institutional affiliations.



Copyright: © 2022 by the authors. Licensee MDPI, Basel, Switzerland. This article is an open access article distributed under the terms and conditions of the Creative Commons Attribution (CC BY) license (<https://creativecommons.org/licenses/by/4.0/>).

1. Introduction

Cemented paste backfill (CPB) is a method that transports the mixture of tailings and cement to the goaf, which can not only deal with pollution and land occupation by tailings, but also may improve ground stability and increase ore recovery [1,2]. This approach has societal, economic, and environmental benefits; thus, CPB has been adopted in many mines worldwide [3–6]. The stability afforded by CPB is key to safe production in mines; therefore, many studies have evaluated the stability of CPB by investigating the material or stope parameters through experiments or numerical simulations [7–11].

The design of CPB helps to provide a safe working environment for underground mining, cuts costs, and improves mineral production [12,13]. In the design of CPB, the interaction between backfill and rock mass is a key element that requires particular attention [14,15]. In particular, understanding the deformation of backfill and rock mass is key to evaluating their interaction—this interaction can be obtained through field measurements, experimental tests, numerical simulations, and other methods, and significant progress has been made in this regard [16,17]. The evolution of displacements between backfill and rock affects the stress magnitude and distribution; thus, analyzing these displacements and stresses also forms the basis of analyzing the interaction between backfill and rock.

Unexpected stress increases and redistributions have been observed in the stope after backfilling, indicating that system evolution through time should be considered. The

underlying reasons for the unexpected stress increases might be the high temperature or the creep behavior of rock mass (CBRM) [18–20]. CBRM refers to the phenomenon that the deformation (or strain) of rock mass increases over time when stress and temperature remain constant. The CBRM effect could be evident when soft rock mass or deep mining depth are encountered. Based on our previous work, unexpected increases in stress could be well explained by emphasizing the role of CBRM and analyzing the interactions between backfill and the surrounding rock mass [6].

It has been found that the number of backfill layers would influence the stress distribution in the backfill materials [21]. For layered backfill, though several works have been undertaken in the past, they were limited to experimental investigation of backfill samples with respect to their mechanical properties [22–24]. Some other studies have investigated the stress state of stopes by considering the different number of layered backfill by numerical simulations. Moreover, many studies have shown that the filling interval time (FIT) and backfill strength are essential factors that affect the magnitude and distribution of stress in the stope [21,25–27]. In the above-mentioned studies, the influence of backfill layering, FIT, and backfill strength was investigated when the rock mass was modeled as elastoplastic [21,28], which cannot reflect the CBRM and time-dependent characteristics of backfill. To date, no research has been conducted that investigates the coupled effect of backfill layering, FIT, and backfill strength when the CBRM is considered.

In this paper, numerical models were developed in Fast LaGrange Analysis of Continua (FLAC^{2D}) software to illustrate the influence of various factors, including layered backfill, FIT, and backfill strength, with a focus on CBRM. By comparing a Burgers-creep viscoplastic model (CVISC) with the Mohr–Coulomb model (MC), the essential differences between the two were determined. The study’s results will contribute to the stope stability evaluation by providing a more reliable and practical numerical modeling framework, which can be used in other similar fields of mining.

2. Methods

The deformation behavior of an unsupported stope was modeled numerically using FLAC^{2D} 8.0 (Itasca, MN, USA), which is a two-dimensional explicit finite-difference program for engineering mechanics computation. Initially, the required inputs for the numerical model were determined, including stope geometry, strength properties of the rock units and contact zones (i.e., interfaces), and the initial stresses. The MC model was then set up based on the previously determined rock properties and configuration as a reference input. A comparison between CVISC and MC models was made to investigate probable variations of the geological features around the stope with time. The simulated deformation magnitudes and patterns of the stopes in the CVISC and MC models were finally compared to determine the extent to which each parameter affected the deformation characteristics.

2.1. Model Inputs

2.1.1. Geometry and Mesh

Figure 1 shows a typical vertical stope of 15 m width and 40 m height, in addition to the size of the whole model, which was determined by testing multiple sizes to find the optimal configuration. The whole model size selected was the configuration that minimized the calculation time while ensuring that the boundary effect did not affect the simulation results.

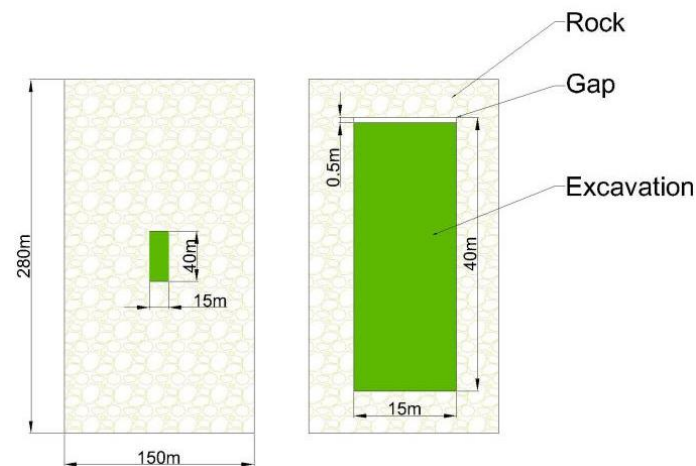


Figure 1. Schematic view of a typical vertical backfilled stope built with FLAC^{2D}.

A preliminary scheme of modeling with FLAC is important to determine a valid mesh arrangement. A mesh size that is too coarse may lead to large deviations from the actual results, whereas an overly dense mesh may unnecessarily increase calculation and make the stress convergence more difficult [21]. Therefore, the mesh is as coarse as possible without affecting the simulation results. This evaluation was implemented early in this investigation by calculating various mesh sizes to select the optimum configuration (detailed results not shown here). The accuracy of the simulation results and the efficiency of the calculation needed to be improved concurrently; therefore, subgrids (the region of rock and backfill) were linked by an attach command to get more precise results using a reasonable grid density arrangement.

As shown in Figure 2, the optimal configuration used 150×280 elements in the peripheral regions (1 m grid size) and 1200×3200 elements in the central region (0.25 m grid size). As it is difficult to achieve complete backfill in practice due to the effects of drainage, consolidation, and cemented backfill desiccation, a 0.5 m gap was left in the model above the backfill surface.



Figure 2. Schematic diagram of grid density division.

2.1.2. Material Properties

To simulate the stability of stope over time, the rock mass was modeled using the MC and CVISC criteria and the backfill was only modeled using the MC criterion. The backfill parameters are shown in Table 1, while the rock mass properties for a reference case are summarized in Tables 2 and 3. These properties were chosen on account of values used in the literature [6].

Table 1. Mohr–Coulomb parameters of the backfill material used in the numerical simulations.

Formation	ρ (Kg/m ³)	K (MPa)	c (MPa)	ϕ (°)	ψ (°)	E (MPa)	G (MPa)
Backfill	18.00	8.33×10^4	20	30	0	150	62.5

Table 2. Mohr–Coulomb parameters of rock mass used in the numerical simulations.

Formation	ρ (Kg/m ³)	K (MPa)	c (MPa)	ϕ (°)	ψ (°)	E (MPa)	G (MPa)
Backfill	25.00	2.64×10^4	5.5	57	0	0.66	1.22×10^4

Table 3. CVISC parameters of rock mass were used in the numerical simulations.

Burgers-Creep Model Parameters	Value	Mohr–Coulomb Model Parameters	Value
K (MPa)	2.64×10^4	c (MPa)	5.5
G_M (MPa)	1.22×10^4	ϕ (°)	57
η_M (Pa·s)	1×10^{20}	ψ (°)	0
G_K (MPa)	1.22×10^4	σ_t (MPa)	0.66
η_K (Pa·s)	1×10^{20}	ρ (Kg/m ³)	25.00

To consider the variational characteristics of backfill over time, the following functions were used to account for the increase in Young's modulus and cohesion:

$$E_b = \begin{cases} 150 & t \leq 8 \\ 415.71 \times \ln(t) - 630.81 & t > 8 \end{cases}$$

$$C_b = \begin{cases} 20 & t \leq 8 \\ 55.4 \times \ln(t) - 84.1 & t > 8 \end{cases}$$

where t represents time in hours, E_b is Young's modulus in MPa, and C_b is cohesion in kPa. These functions were obtained through the literature [6].

For numerical modeling, when the rock mass and backfill were assumed to behave as Mohr–Coulomb materials, the rock region was initially allowed to reach equilibrium under its self-weight; the stope was then excavated with FLAC^{2D} calculations until an equilibrium state was reached. In the same way, the rock mass was modeled using the MC criterion and the results were obtained after an equilibrium state was reached.

The major difference between CVISC and MC models in FLAC is related to the time in the numerical simulation. The 'step' represents the calculation step in the MC model; in the CVISC model, this represents actual time [15]. The CVISC model, namely Burger's viscoplastic behavior model, was extensively used to investigate CBRM. The advantage of this model is that the Burger's creep effect is expressed in the rock mass, and the Mohr–Coulomb criterion is adopted for the plastic failure of rock mass, which is more in line with the characteristics of deformation failure of weakly cemented soft rock. To avoid the unstable results in the CVISC model, a time step needs to be set to ensure that the increment of stress over time should be small enough compared to the strain-dependent stress increment [29]. The system was in different mechanical equilibrium states over time. Interested readers could refer to [6,29] for detailed information about MC and CVISC constitutive models, which are not covered in the current study for clarity purposes.

The CVISC approach has been widely used in FLAC^{2D} and has been well implemented in CBRM. For example, the CVISC method was used by Bonini et al. [30], who constructed a visco-elastoplastic creep model of clay shales to improve the description of the time-dependent behavior of this lithology. Sharifzadeh et al. [29] utilized the CVISC model and found that numerical results were basic coincidence with measured in situ displacements. Qi and Fourie [6] indicated numerical simulation using the CVISC model could accurately describe the CBRM by simulating the horizontal displacement of the stope in Baixiangshan Iron Mine, An-hui, China.

2.1.3. Initial Stresses

The initial stresses are related to the overburden weight (500 m above the numerical model) and the ground pressure coefficient ($\sigma_h/\sigma_v = 2$). Initial stresses were calculated as follows: $\sigma_{yy} = 32$ MPa, $\sigma_{xx} = 64$ MPa, and $\sigma_{zz} = 64$ MPa.

2.2. Modeling Procedure

Each numerical simulation had four steps:

1. After the model geometry and mesh configuration were set, the boundaries and initial stress state were input into the numerical model. The bottom boundaries of the model were fixed in the vertical direction, while the left and right boundaries were fixed in the horizontal directions. The unexcavated model was initially equilibrated elastically to let the formations settle down as they were loaded. Appropriate positions were set to monitor displacement and stress evolution.

2. The stope was excavated, and the MC or CVISC criterion was used in the rock mass. When the rock mass and the backfill were modeled using the MC criterion, excavation of the whole stope was completed first; thus, it can be supposed that no further convergence would take place in the rock mass walls when backfill was placed in the stope. After excavation, the corresponding model step was run and the stope re-evaluated; in other words, the stope was filled without waiting for stress balancing to complete. When the CVISC criterion was assigned to the rock mass and the MC criterion was assigned to the backfill, the position and stress of the rock mass changed with time.

3. The stope was backfilled in single or several steps considering different FIT and backfill strength values.

4. The numerical simulation was run for 32 days (including the FIT) after filling commenced to investigate the evolution of displacement and stress distribution in backfilled stopes. The authors note that the CVISC model has been well validated for the simulation of mine backfill in our previous work [6].

3. Results and Discussion

3.1. Initial Model

Two different cases were established for comparison. The rock mass in Case 1 was modeled with MC, whereas the rock mass of Case 2 was modeled with CVISC. For the reference case, Figure 3a,b plots the stress evolution (the backfilling center—see the red dots in Figure 3), and Figure 3c,d plots displacements of the rock mass (the backfilling side and top—see red dots in Figure 3) through time. The stress was found to increase with time, with the rate of increase faster in the early stages after backfilling in Case 2. The rate of the first three days was particularly fast, with increases accounting for 55.0% and 61.7% of the total horizontal and vertical stresses, respectively, occurring during this period. The horizontal displacement rate during the first 7 days was 1.76 cm/day, which was much higher than the average displacement rate from Day 8 to Day 32 (0.31 cm/day).

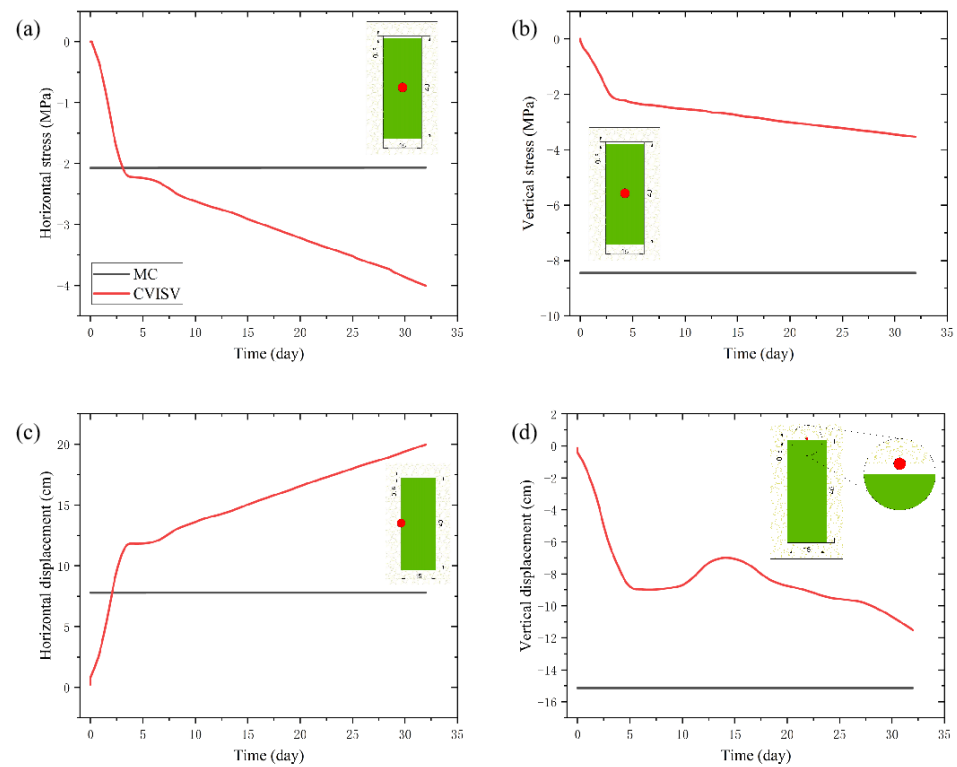


Figure 3. Time-dependent response in the reference case: (a) horizontal, (b) vertical stress versus time, (c) horizontal, and (d) vertical displacement versus time.

As shown in Figure 3, the change in rock mass was rapid in the early stages after filling and became slower in the later period. As described in previous literature [31], the evolution of rock mass damage rate (i.e., frequency derivative of the rock mass damage factor with time) decayed with time, which is interpreted to be the cause of the observed phenomenon. In our previous study, the rock mass was found to move inward with time, which is the basic distinction between the MC model compared with the CVISC model [6]. Therefore, the CBRM is vital to investigate the evolution of stress and displacement over time in backfilled stopes.

3.2. Different Layers of CPB

As described above, the CVISC or MC criterion was assigned to the rock mass and the MC criterion was assigned to the backfill in all cases. According to the actual backfill situations in the mine sites, three simulation scenarios were designed, as shown in Figure 4.

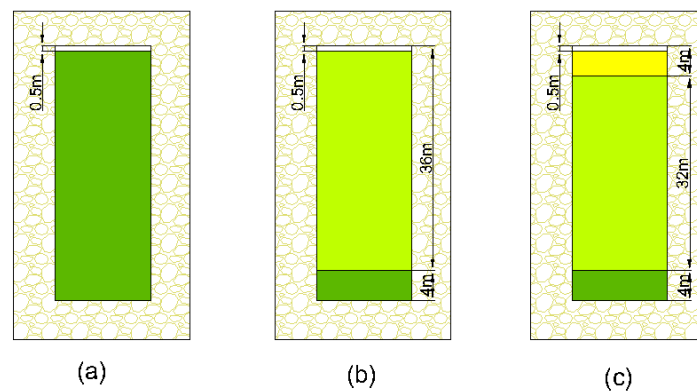


Figure 4. Different layers of cemented paste backfill case: (a) Case 1 (backfilled in a single step); (b) Case 2 (backfill in two steps); (c) Case 3 (backfill in three steps).

3.2.1. CVISC Model

The influence of backfill layer placement on the stress evolution is shown in Figure 5a,b. As shown, the peak vertical and horizontal stresses of Cases 2 and 3 were higher than those of Case 1. In contrast to the layered backfill, the entire backfill was relatively constrained when placed in a single step, as shown in [32]. This tendency resulted in an increase in shear stress at the interface between backfill and rock mass and a reduction of the vertical and horizontal stresses in CPB [33]. Meanwhile, the stress in the slope center using the multiple filling layer approach was found to fluctuate more strongly than using a single filling step (as shown in Figure S1 in Supporting Materials). This indicates that backfill placement might influence stress distribution [34].

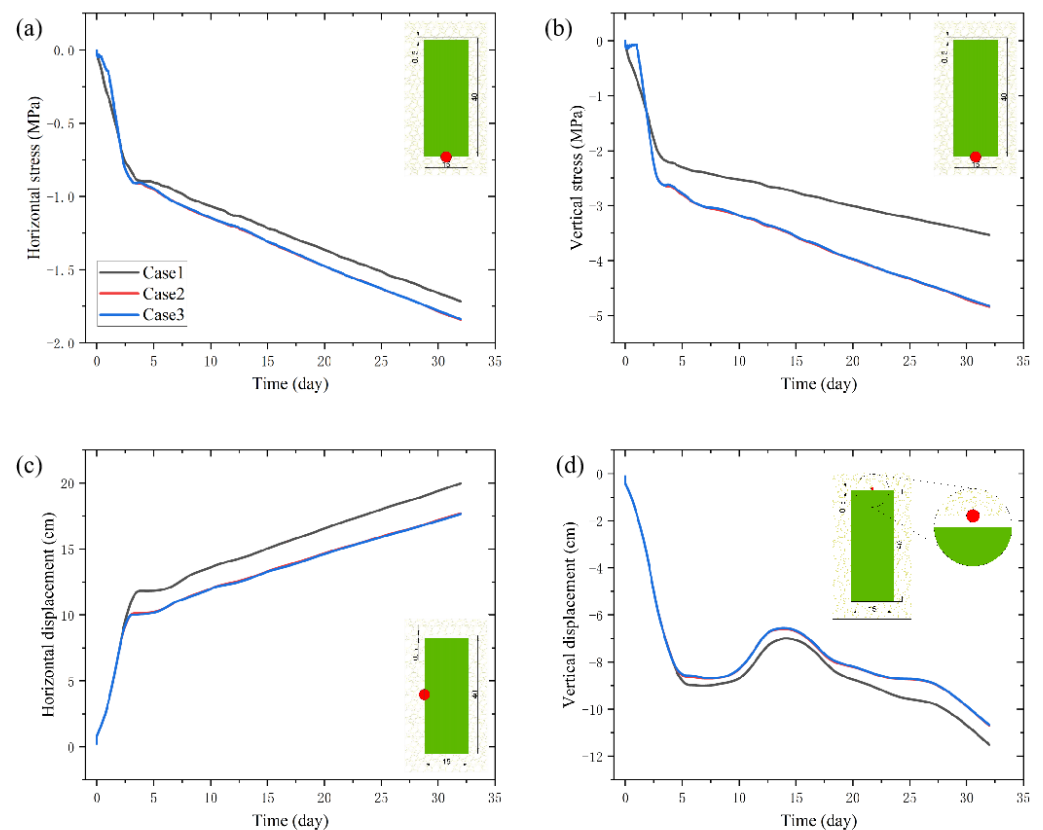


Figure 5. The influence of backfill layers on the (a) horizontal stresses, (b) vertical stresses, (c) horizontal displacement, and (d) vertical displacements evolution on the monitoring point (see the red dot in Figure 5).

Figure 5c,d reveals the evolution of displacement with different backfill layers. The horizontal displacement near the middle position of the backfilled slope edge and the vertical displacement at the top of the slope in Case 1 was the largest. However, the horizontal and vertical displacements in Cases 2 and 3 were relatively small, with only minimal distinction between cases. The slope was backfilled in a single step, which generated a significant impact load until the stress reached a stable state. The abrupt backfill caused high horizontal stress in the slope [21], which is interpreted as the influence of layering on horizontal displacements.

The rapid increase in horizontal and vertical displacements in Case 1 lasted longer than that of Cases 2 and 3, as shown in Figure 5c,d. The evolution of horizontal and vertical displacements with different layers was consistently slow in the later period after filling. The inflection point between rapid and slow displacement rates varied, leading to differences in the horizontal and vertical displacements of different layers. The self-weight of the backfill in the single step provides a possible explanation for the high horizontal

and vertical displacements. When the rock mass was modeled using the MC approach, the horizontal and vertical displacements of the backfilled stope were larger than those of the unfilled stope (as shown in Figure S2, Supporting Materials); therefore, the self-weight of the backfill affected the displacement evolution of the rock mass. The influence of backfill self-weight lasted longer when backfilled stope in a single step in CVISC, which increased the horizontal and vertical displacement (Figure 5). Moreover, the increase in the number of backfill placement layers reduced transverse deformation of the rock mass (as shown in Figures S3 and S4, Supporting Materials) because of the unfilled goaf above. It should be noted that placement of the entire backfill reduced the degree of inward displacement of the rock mass; however, the effect was weak in comparison to the influence of the backfill self-weight.

As shown in Figure 6, the stress in the stope was smaller in Case 1 than in Cases 2 and 3, which is consistent with the results shown in Figure 5a,b. The stresses in the lower part of the backfilled stope were influenced when the stope was backfilled in several layers. Compared to Case 2, greater stresses in the surrounding rock mass around the stope were observed in Case 1. Although there were no significant differences observed between Cases 2 and 3, an extremely small stress increase within the stope was observed in Case 3. The above results show that the stress within the stope increased with an increasing number of backfill layers, as demonstrated in Figure 5. In contrast, the stress in the surrounding rock mass was higher in Case 1 compared with Cases 2 and 3, which was caused by the stress redistribution.

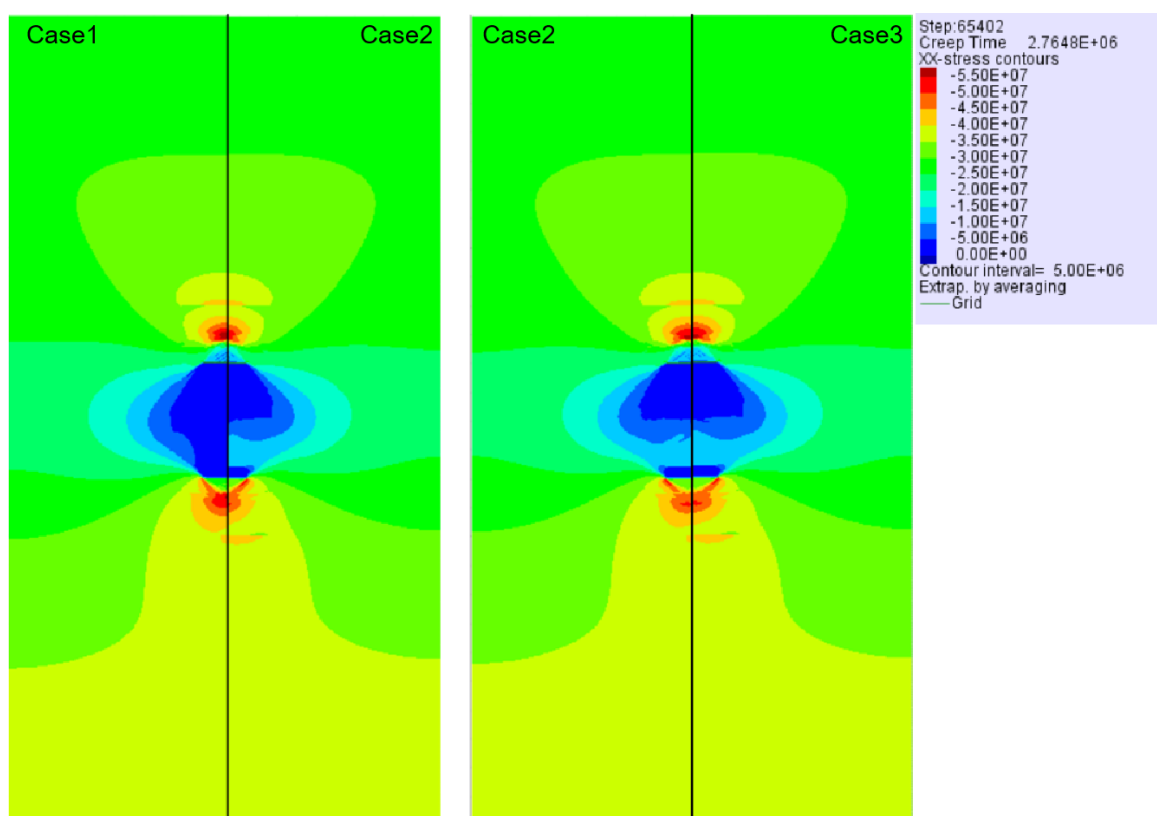


Figure 6. Stress distribution at 32 days with different backfill layers.

As shown in Figure 7, the elastic deformation area and range of shear or volume yield were larger when the stope was backfilled several times. The shear or volume yield was highly concentrated in the lower part of the stope in Case 1; in contrast, evident yield in the middle or upper part of the stope was also observed in Cases 2 and 3. However, the plastic deformation area within the stope in Case 3 was distributed more uniformly. The results in

Figure 7 correspond well to the stress distribution shown in Figure 6, i.e., the broader the stress distribution within the stope, the larger the plastic deformation area.

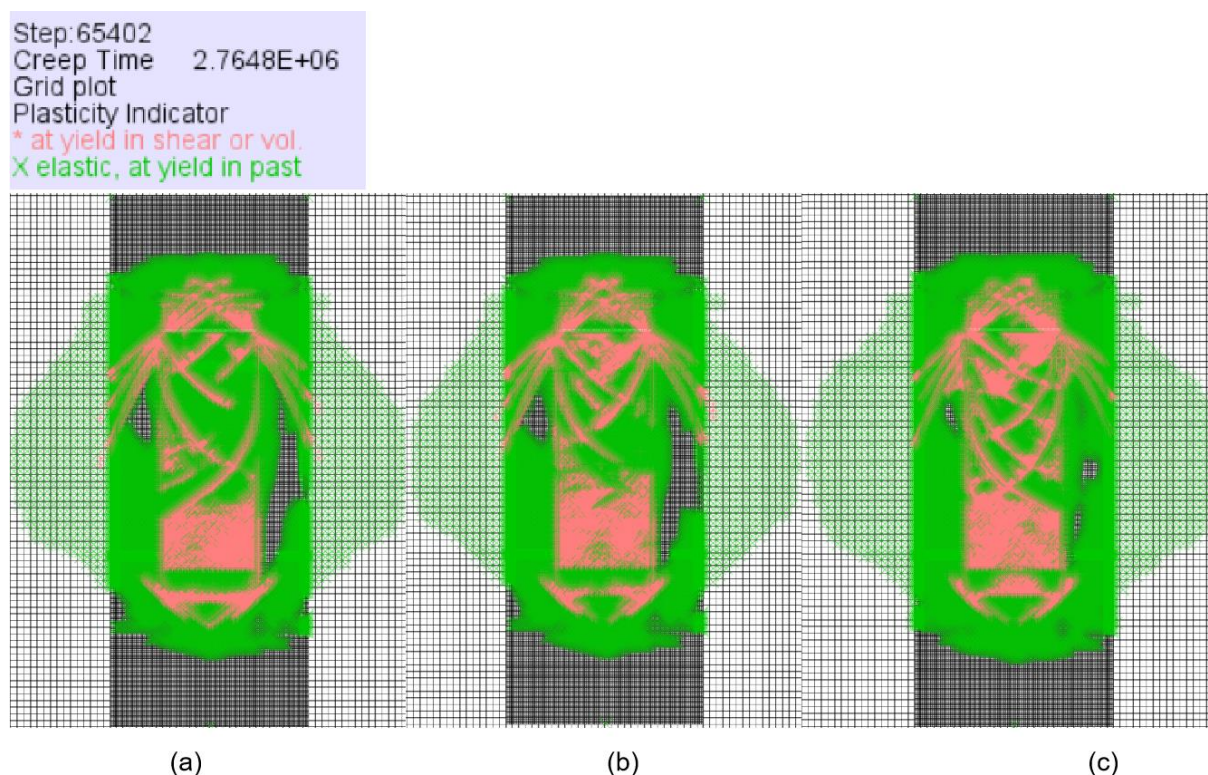


Figure 7. Elastic and plastic region within the backfilled stope at 32 days with different backfill layers: (a) Case 1, (b) Case 2, and (c) Case 3.

During inward displacement of the rock mass, slip and dislocation inside the backfill or layered backfill occurred, which caused backfill instability or failure. Therefore, the backfill failure process was essentially a process of continuous development, expansion, and collection of damage under the coupled effects of delamination and loading [22]. In summary, backfilling one or several times affected the plastic deformation in the middle and upper parts of the backfilled stope but had a slight influence on the stress distribution in the lower part. The damage region expanded because of increasing backfill stress and slip and dislocation between backfill layers.

3.2.2. Comparison between CVISC and MC Models

In this section, the results of assigning the CVISC and MC models to the rock mass are compared. Figure 8 illustrates the stresses around the center and bottom-middle part of the backfill at day 32 under both CVISC and MC modeling approaches. The stress deviations caused by the backfilling layers were large in the MC scenarios, as shown in Figure 8a. Stresses obtained in the single-layer backfill were overestimated in the MC model, as suggested in [21]. In contrast, the stress in a single step was close to the stress state modeled in multiple steps using the CVISC approach. Because of the inaccurate results of the single-layer backfill with the MC model, this type of modeling procedure is not recommended in future studies. Taking into consideration the inaccuracy of the single-layer backfill with MC, the stresses using the CVISC model were larger than using the MC due to the continuous rock mass deformation in CVISC.

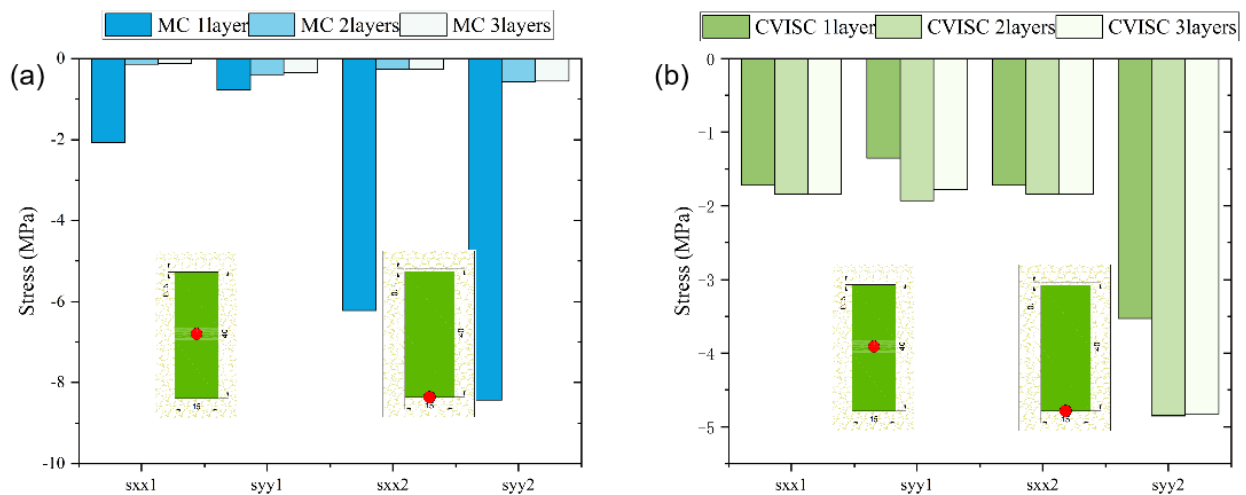


Figure 8. The stress difference between (a) MC and (b) CVISC constitutive models of the rock mass.

3.3. Filling Interval Time

During layered backfilling using the MC model, the next layer was placed when a stress balance was achieved. Therefore, there is no ‘time’ concept for the filling interval when the rock mass was modeled using MC. In this section, the effect of filling interval time was investigated using the CVISC scenarios. The slope was backfilled in three layers, with heights of 4 m, 32 m, and 4 m height, in all scenarios. The FIT values were selected to be 24 h, 36 h, and 48 h.

The stress evolution with different FIT values is shown in Figure 9a,b. As illustrated, the vertical and horizontal stresses were minimal when the FIT was 48 h, which is in good agreement with the results described in [6]. A larger FIT represents less available time for the stress distribution from the rock mass to transfer to the backfilled stope, especially under rapid displacement periods of the rock mass. Therefore, the stress within the stope was smaller when the FIT was increased.

Figure 9c,d presents the influence of FIT on the evolution of displacements. Note that time measurements started when the stope was initially backfilled and included the FIT. As shown, the horizontal and vertical displacements increased with increasing FIT. The interpretation of the above results is straightforward—a larger FIT means a longer time period during which the rock mass can displace relatively freely. Therefore, the longer the FIT, the greater the degree of inward displacement of the rock mass [28].

The area of elastic deformation and yield within the backfill increased with the FIT, as shown in Figure 10. A possible reason for this observation is that increasing FIT caused a failure mode change from tensile failure to tensile shear failure, and then to mixed tensile and shear failure of the backfill [35]. Due to the continuous displacement of rock mass, the plastic area within the stope increased to a certain extent, which might cause failure of the stope [36]. Therefore, to avoid expansion of the plastic region, the FIT should be minimized during backfilling.

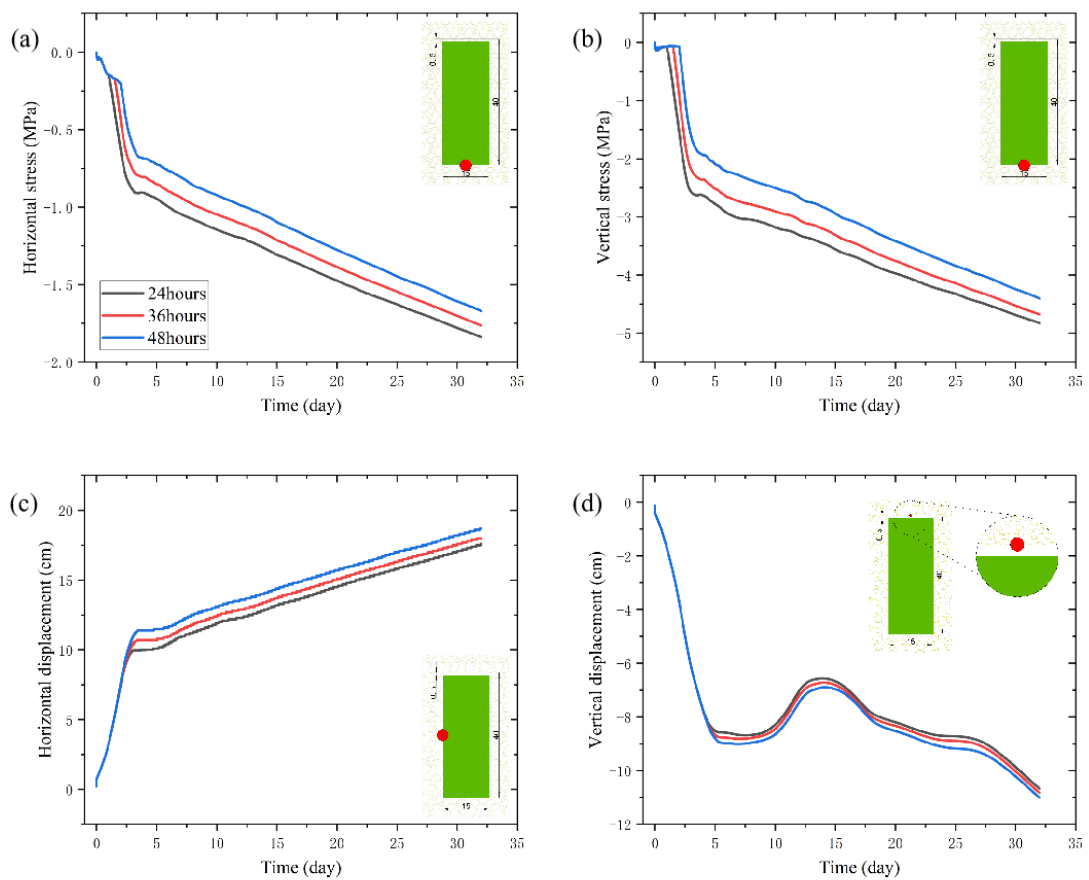


Figure 9. Stresses and displacements evolution with different FIT values (24 h, 36 h, and 48 h): (a) horizontal stresses, (b) vertical stresses, (c) horizontal displacement, and (d) vertical displacements, on the monitoring point (see the red dot in Figure 9).

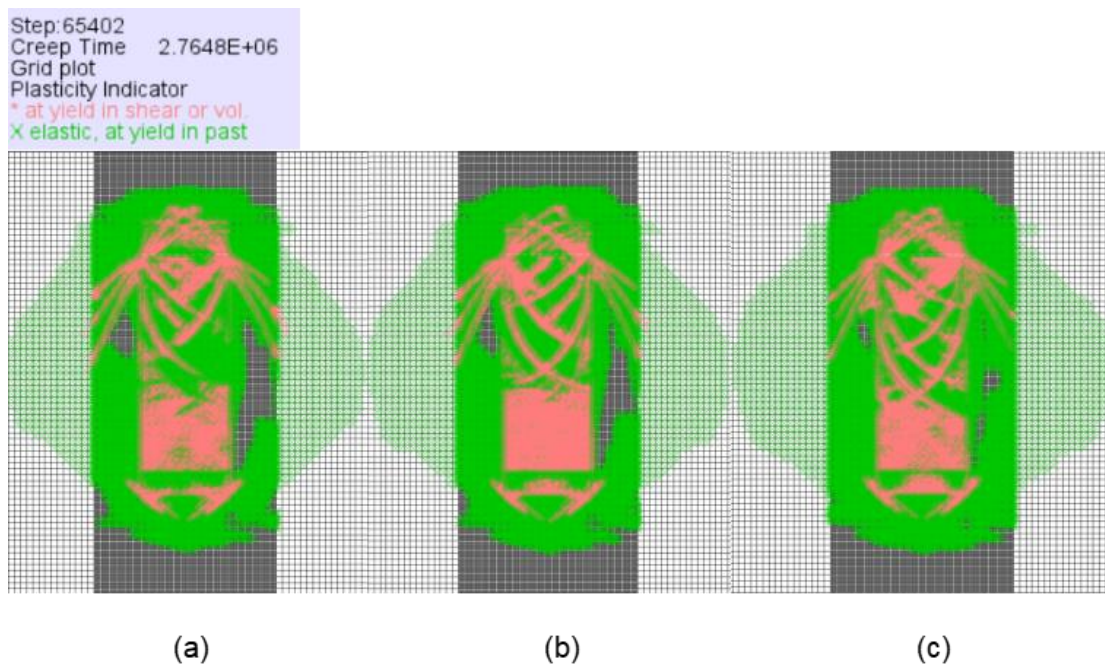


Figure 10. Elastic and plastic region within the backfilled stope at 32 days with different FIT values; (a) the FIT is 24 h, (b) 36 h, and (c) 48 h.

3.4. Different Strength

In this section, the influence of backfill strength on the interaction of rock mass and backfill was investigated. The stope was backfilled in three layers (the fill heights were 4 m, 32 m, and 4 m) but assigned with different strength parameters for the central layer. Based on actual implementation in mines, the upper part of the stope as a mining face and the lower part of the stope to prevent water penetration both require high strength. According to the preliminary tests, stable stress results could be obtained when the strength of the middle backfill was greater than half that of the bottom or top. Therefore, the ratios between middle strength and bottom strength chosen for testing were determined to be 0.5, 0.6, 0.7, 0.8, 0.9, and 1.

Figure 11c,d shows the influence of strength on displacement. When the strength of the backfill in the middle part decreased, the horizontal and vertical displacements increased. Hooke's law illustrates that a decrease of the elastic modulus leads to a strain increase. The backfill strength was represented by the elastic modulus and the shear modulus; the lower the backfill strength, the greater the backfill strain under the same stress environment. Therefore, the rock mass displacement is larger when the backfill strength decreases.

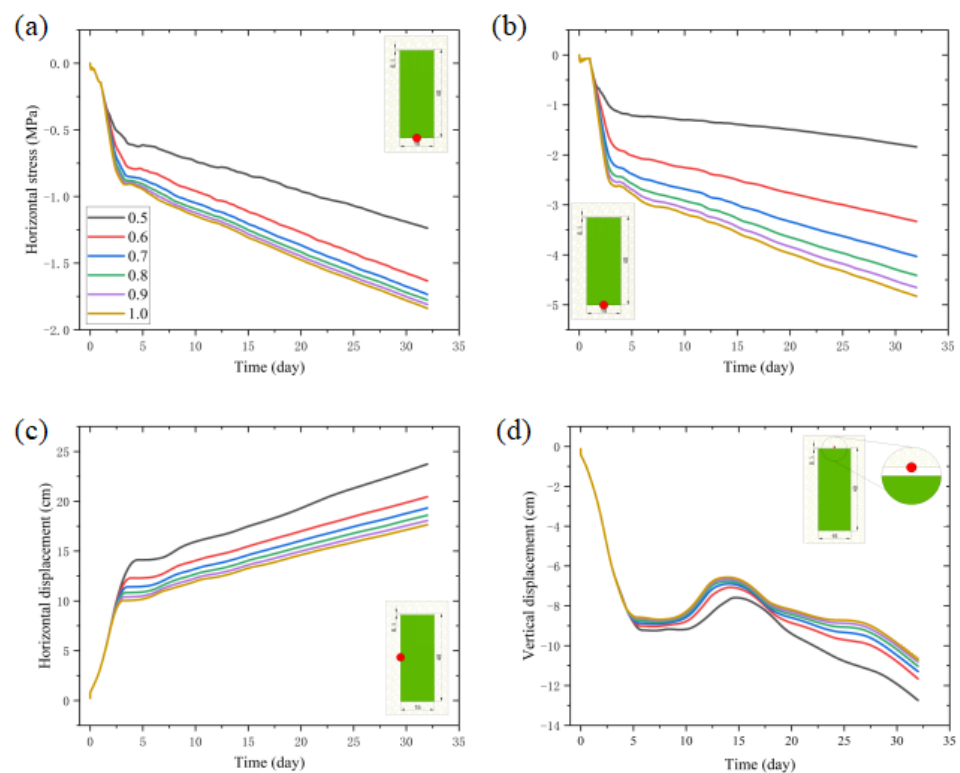


Figure 11. Effect of backfill strength on the stress and displacement distribution: (a) horizontal stresses, (b) vertical stresses, (c) horizontal displacements, and (d) vertical displacements.

As shown in Figure 11a,b, the vertical and horizontal stresses on the bottom stope decreased when the strength of the middle backfill decreased. Creep damage processes absorbed and dissipated substantial amounts of energy [37]. The reason for the lower stress with lower strength backfill might be that the rock mass creep damage process absorbed and dissipated more energy because of serious strain. Moreover, the lower backfill strength indicates its lower capacity to store energy without damage. Once severe damage occurs in the backfill, the stress would redistribute to rock mass.

Figure 12 indicates the influence of strength improvement of backfill on stope stability. As shown in Figure 12, the region of elastic deformation and shear yield expanded when the middle backfill strength decreased. Therefore, stope stability requires a certain strength of backfill.

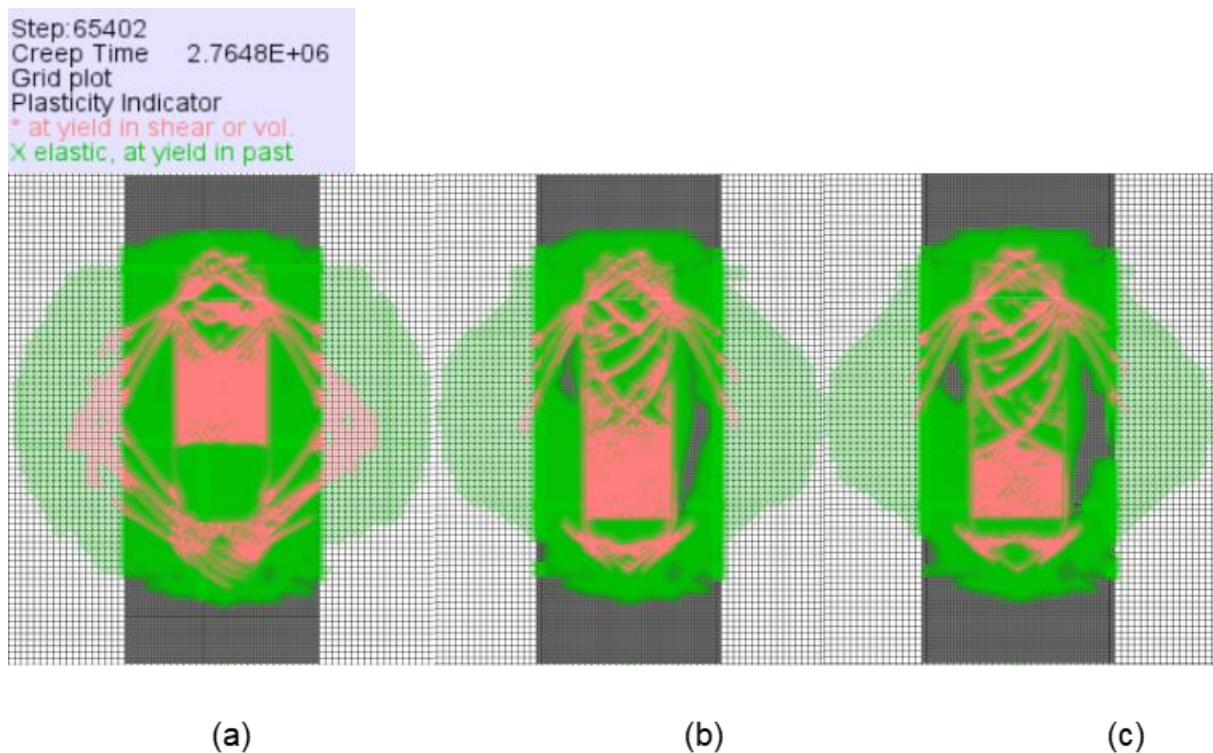


Figure 12. Plastic strain distribution in the backfilled stope at 32 days with different strength (a) 0.5, (b) 0.7, and (c) 0.9 of the middle-backfilled stope (coefficient in Figure 11 is the strength in the middle backfill accounts for the strength in the top and bottom).

4. Conclusions

In this paper, a numerical model was established taking the MC model as a reference; the interactions between rock mass and backfill were then analyzed by considering the CBRM. The CBRM explained the continuous inward movement of the rock mass with time. The numerical model evaluated the stability of the stope by considering the evolution of stope displacements and stresses. In addition to the reference case, a parametric study was conducted to investigate the influence of backfill layers, FIT, and backfill strength on the stability of the stope.

(1) The vertical stress at the bottom of the stope was greater than the horizontal stress in CVISC. The vertical and horizontal stress of the backfilled stope in single steps were smallest using CVISC, while horizontal displacement near the middle position of the backfilled stope edge and vertical displacement at the top of the backfilled stope was largest. The horizontal and vertical displacements of the stope backfilled in multiple steps were relatively small with minimal distinction. When using the MC model for the rock mass, the backfill step influence on stress was more significant than for the CVISC model. The stresses using CVISC were larger than those obtained using MC due to continuous deformation of rock mass deformation in the CVISC model.

(2) The increase of FIT had a greater impact on stress and less impact on displacement. For the stress at the bottom of the stope, the stress was smaller when the FIT was increased. The horizontal and vertical displacements both increased with increasing FIT.

(3) The vertical and horizontal stresses at the bottom of the stope decreased when the strength of the backfill decreased. When the strength of the backfill in the middle part decreased, the horizontal and vertical displacements increased, and the region of the elastic deformation and shear yield expanded.

5. Future Work

In the future, other important factors, such as pore water pressure and drainage, need to be considered during numerical simulations. Moreover, the excavation and backfilling of two adjacent stopes could be a worthwhile topic for further investigation, since it is more related to in situ practices, especially considering CBRM. Because the height and interval of the layered backfilling were different, if the middle or upper part of the stope was selected as the stress monitoring point, the stress would not have been fully detected until filling had been completed. Therefore, we selected the bottom of the stope as the stress monitoring point; however, the stress at the bottom of the stope may not fully reflect the stress impact of the CBRM on the stope as a whole. Thus, future modeling could potentially monitor stress conditions at multiple locations throughout the stope.

Supplementary Materials: The following supporting information can be downloaded at: <https://www.mdpi.com/article/10.3390/min12020271/s1>, Figure S1: The influence of backfill layers on the (a) horizontal stress and (b) vertical stress on the central stope (see the red dot in S1); Figure S2. Difference of horizontal and vertical displacement after the excavation and backfill in MC; Figure S3. Different layers of cement paste backfill case: (a) backfill in a single step; (b) backfill in two steps; (c) backfill in three steps (d) backfill in four steps and (e) backfill in six steps; Figure S4. The influence of different backfill layers (see the S2) on the (a) horizontal displacement and (b) vertical displacement on the monitor point (see the red dot in S3).

Author Contributions: For research articles with several authors, the following statements should be used Conceptualization, C.Q. and Q.C.; methodology, L.G.; software, L.G.; validation, C.Q., Y.W. and Q.Z.; formal analysis, L.G.; writing—original draft preparation, C.Q. and L.G.; writing—review and editing, All authors; visualization, L.G.; supervision, C.Q.; funding acquisition, C.Q. All authors have read and agreed to the published version of the manuscript.

Funding: This research was funded by State Key Laboratory for GeoMechanics and Deep Underground Engineering, China University of Mining & Technology (No. SKLGDUEK2002).

Acknowledgments: This work is Supported by State Key Laboratory for GeoMechanics and Deep Underground Engineering, China University of Mining & Technology (No. SKLGDUEK2002).

Conflicts of Interest: The authors declare no conflict of interest.

Abbreviations

CBRM	Creep behavior of the rock mass
CVISC	Burger-creep viscoplastic model
CPB	Cemented paste backfill
FIT	Filling interval time
MC	Mohr–Coulomb model
ρ	Density
G	Shear modulus
η	Viscosity
K	Bulk modulus
E	Young's modulus
ϕ	Interface friction angle
μ	Poisson's ratio
c	Cohesion
ψ	Dilation angle

References

1. Brackebusch, F.W. Basics of paste backfill systems. *Min. Eng.* **1994**, *46*, 1175–1178.
2. Benzaazoua, M.; Ouellet, J.; Servant, S.; Newman, P.; Verburg, R. Cementitious backfill with high sulfur content Physical, chemical, and mineralogical characterization. *Cem. Concr. Res.* **1999**, *29*, 719–725. [[CrossRef](#)]
3. Chen, Q.; Zhang, Q.; Qi, C.; Fourie, A.; Xiao, C. Recycling phosphogypsum and construction demolition waste for cemented paste backfill and its environmental impact. *J. Clean. Prod.* **2018**, *186*, 418–429. [[CrossRef](#)]

4. Edraki, M.; Baumgartl, T.; Manlapig, E.; Bradshaw, D.; Franks, D.; Moran, C.J. Designing mine tailings for better environmental, social and economic outcomes: A review of alternative approaches. *J. Clean. Prod.* **2014**, *84*, 411–420. [[CrossRef](#)]
5. Benzaazoua, M.; Bussi re, B.; Demers, I.; Aubertin, M.; Fried,  .; Blier, A. Integrated mine tailings management by combining environmental desulphurization and cemented paste backfill: Application to mine Doyon, Quebec, Canada. *Miner. Eng.* **2008**, *21*, 330–340. [[CrossRef](#)]
6. Qi, C.; Fourie, A. Numerical Investigation of the Stress Distribution in Backfilled Stopes Considering Creep Behaviour of Rock Mass. *Rock Mech. Rock Eng.* **2019**, *52*, 3353–3371. [[CrossRef](#)]
7. Kesimal, A.; Yilmaz, E.; Ercikdi, B.; Alp, I.; Deveci, H. Effect of properties of tailings and binder on the short-and long-term strength and stability of cemented paste backfill. *Mater. Lett.* **2005**, *59*, 3703–3709. [[CrossRef](#)]
8. Yang, P.; Li, L.; Aubertin, M.; Brochu-Baekelmans, M.; Ouellet, S. Stability Analyses of Waste Rock Barricades Designed to Retain Paste Backfill. *Int. J. G om ch.* **2017**, *17*, 04016079. [[CrossRef](#)]
9. Cui, L.; Fall, M. Numerical Simulation of Consolidation Behavior of Large Hydrating Fill Mass. *Int. J. Concr. Struct. Mater.* **2020**, *14*, 23. [[CrossRef](#)]
10. Li, G.; Sun, Y.; Qi, C. Machine learning-based constitutive models for cement-grouted coal specimens under shearing. *Int. J. Min. Sci. Technol.* **2021**, *31*, 813–823. [[CrossRef](#)]
11. Qi, C.; Xu, X.; Chen, Q. Hydration reactivity difference between dicalcium silicate and tricalcium silicate revealed from structural and Bader charge analysis. *Int. J. Miner. Met. Mater.* **2022**, *29*, 335–344. [[CrossRef](#)]
12. Belem, T.; Benzaazoua, M. Design and Application of Underground Mine Paste Backfill Technology. *Geotech. Geol. Eng.* **2007**, *26*, 147–174. [[CrossRef](#)]
13. McLellan, B.; Corder, G.; Giurco, D.; Green, S. Incorporating sustainable development in the design of mineral processing operations—Review and analysis of current approaches. *J. Clean. Prod.* **2009**, *17*, 1414–1425. [[CrossRef](#)]
14. Jafari, M.; Shahsavari, M.; Grabinsky, M. Drained Triaxial Compressive Shear Response of Cemented Paste Backfill (CPB). *Rock Mech. Rock Eng.* **2021**, *54*, 3309–3325. [[CrossRef](#)]
15. Fang, K.; Fall, M. Shear Behaviour of Rock–Tailings Backfill Interface: Effect of Cementation, Rock Type, and Rock Surface Roughness. *Geotech. Geol. Eng.* **2021**, *39*, 1753–1770. [[CrossRef](#)]
16. Hassani, F.R.; Mortazavi, A.; Shabani, M. An investigation of mechanisms involved in backfill-rock mass behaviour in nar-row vein mining. *J. S. Afr. Inst. Min. Metall.* **2008**, *108*, 463–472.
17. Kosakowski, G.; Berner, U. The evolution of clay rock/cement interfaces in a cementitious repository for low- and inter-mediate level radioactive waste. *Phys. Chem. Earth* **2013**, *64*, 65–86. [[CrossRef](#)]
18. Thompson, B.; Bawden, W.; Grabinsky, M. In situ measurements of cemented paste backfill at the Cayeli Mine. *Can. Geotech. J.* **2012**, *49*, 755–772. [[CrossRef](#)]
19. Zhang, F.R. Experimental study of damage and creep property of rock under coupled chemical corrosion and freeze-thaw cycle. *Rock Soil Mech.* **2019**, *40*, 3879–3888.
20. Apuani, T.; Masetti, M.; Rossi, M. Stress–strain–time numerical modelling of a deep-seated gravitational slope deformation: Preliminary results. *Quat. Int.* **2007**, *171–172*, 80–89. [[CrossRef](#)]
21. Li, L.; Aubertin, M. Numerical Investigation of the Stress State in Inclined Backfilled Stopes. *Int. J. G om ch.* **2009**, *9*, 52–62. [[CrossRef](#)]
22. Fu, J.; Wang, J.; Song, W. Damage constitutive model and strength criterion of cemented paste backfill based on layered effect considerations. *J. Mater. Res. Technol.* **2020**, *9*, 6073–6084. [[CrossRef](#)]
23. Zhang, Y.-H.; Wang, X.-M.; Wei, C.; Zhang, Q.-L. Dynamic mechanical properties and instability behavior of layered backfill under intermediate strain rates. *Trans. Nonferrous Met. Soc. China* **2017**, *27*, 1608–1617. [[CrossRef](#)]
24. Cao, S.; Song, W.D.; Xue, G.L.; Wang, Y.; Zhu, P.R. Tests of strength reduction of cemented tailings filling considering layering character. *Rock Soil Mech.* **2015**, *36*, 2869–2876.
25. Benzaazoua, M.; Fall, M.; Belem, T. A contribution to understanding the hardening process of cemented pastefill. *Miner. Eng.* **2004**, *17*, 141–152. [[CrossRef](#)]
26. Cao, S.; Song, W. Effect of filling interval time on the mechanical strength and ultrasonic properties of cemented coarse tailing backfill. *Int. J. Miner. Process.* **2017**, *166*, 62–68. [[CrossRef](#)]
27. Cao, S.; Song, W.-d. Effect of Filling Interval Time on Long-Term Mechanical Strength of Layered Cemented Tailing Back-fill. *Adv. Mater. Sci. Eng.* **2016**, *2016*, 9507852. [[CrossRef](#)]
28. Li, L.; Aubertin, M. Numerical Analysis of the Stress Distribution in Symmetrical Backfilled Trenches with Inclined Walls. *Indian Geotech. J.* **2014**, *45*, 278–290. [[CrossRef](#)]
29. Sharifzadeh, M.; Tarifard, A.; Moridi, M.A. Time-dependent behavior of tunnel lining in weak rock mass based on dis-placement back analysis method. *Tunn. Undergr. Space Technol.* **2013**, *38*, 348–356. [[CrossRef](#)]
30. Bonini, M.; Debernardi, D.; Barla, M.; Barla, G.B. The Mechanical Behaviour of Clay Shales and Implications on the Design of Tunnels. *Rock Mech. Rock Eng.* **2007**, *42*, 361–388. [[CrossRef](#)]
31. Lin, H.; Zhang, X.; Cao, R.; Wen, Z. Improved nonlinear Burgers shear creep model based on the time-dependent shear strength for rock. *Environ. Earth Sci.* **2020**, *79*, 149. [[CrossRef](#)]
32. Karaoglu, K.; Yilmaz, E. *Cemented Paste Backfill Pressure Monitoring and Field Testing*; Springer: Cham, Switzerland, 2017; pp. 195–214. [[CrossRef](#)]

33. Li, L.; Aubertin, M.; Belem, T. Formulation of a three dimensional analytical solution to evaluate stresses in backfilled vertical narrow openings. *Can. Geotech. J.* **2005**, *42*, 1705–1717. [[CrossRef](#)]
34. Sobhi, M.A.; Li, L.; Aubertin, M. Numerical investigation of earth pressure coefficient along central line of backfilled stopes. *Can. Geotech. J.* **2017**, *54*, 138–145. [[CrossRef](#)]
35. Wang, J.; Fu, J.; Song, W. Mechanical properties and microstructure of layered cemented paste backfill under triaxial cyclic loading and unloading. *Constr. Build. Mater.* **2020**, *257*, 119540. [[CrossRef](#)]
36. Wu, S.Z.; Wang, M.N.; Yu, L.; Liu, D.G.; Huang, Q.W. Model test study on stress characteristics of backfill to segment in TBM tunnel. *Rock Soil Mech.* **2018**, *39*, 3976.
37. Li, S.; Zhang, R.; Feng, R.; Hu, B.; Wang, G.; Yu, H. Feasibility of Recycling Bayer Process Red Mud for the Safety Backfill Mining of Layered Soft Bauxite under Coal Seams. *Minerals* **2021**, *11*, 722. [[CrossRef](#)]